

Using the Marcus Inverted Region for Rectification in Donor–Bridge–Acceptor “Wire” Assemblies

Norman Sutin,^{*,†} Bruce S. Brunschwig,^{*,‡} and Carol Creutz^{*,†}

Chemistry Department, Brookhaven National Laboratory, Upton, New York 11973-5000,
Beckman Institute California Institute of Technology, Mail Code 139-74, 1200 East California Boulevard,
Pasadena, California 91125

Received: June 2, 2003

We examine the properties of a system in which a hopping mechanism can exploit the nuclear factors, along with the field resulting from the applied voltage, to control the current through a donor–bridge–acceptor (D–B–A) system inserted between two metal electrodes. We find that, by utilizing D/A couples with small λ values, switching can be achieved at modest applied potentials.

Introduction

Molecules are being examined as candidates for electronic wires in nanostructures.^{1–4} Typically a bridging molecule (B) such as 1,4-benzenedithiol is inserted between gold electrodes (M) and a voltage is applied across M–B–M.⁵ Electrons can tunnel across the bridge and, as the applied electric field brings the metal and bridging molecule orbital (LUMO, HOMO) levels to the same energy, resonant tunneling can occur.⁶ In voltage regions far from resonance, a superexchange description of the tunneling includes the electronic energies of the bridge. However, the nuclear factors (λ , ΔG^0) that control the rate of electron transfer in solution⁷ are absent from the description of the system's conductance.⁸ Here we examine the properties of a system in which a hopping mechanism exploits the nuclear factors, along with the field resulting from the applied voltage, to control the current through a donor–bridge–acceptor (D–B–A) system inserted between metal electrodes. We find that, though they exhibit Ohmic behavior and positive differential conductances at small applied voltages, even formally symmetrical D–B–A systems may show *negative* differential conductances as a consequence of their being in the inverted region at greater driving force. This has important implications, which, so far as we are aware, have not generally been appreciated.

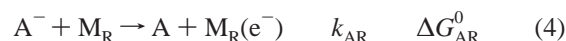
Results and Discussion

Consider an M|D–B–A|M assembly in which a neutral D–B–A serves as a wire connecting two metal electrodes.^{9–11} No electrolyte is added and the electronic coupling between the D and A sites is moderate (such that electron transfer is borderline adiabatic, with the electron trapped at D and A, not delocalized over the two sites). Electron transport through D–B–A proceeds via parallel tunneling (k_{tun}) and hopping (k_{hop}) processes and the net electron-transfer rate constant k_{et} is given by the sum

$$k_{\text{et}} = k_{\text{tun}} + k_{\text{hop}} \quad (1)$$

We focus on the case where an electron-hopping mechanism dominates. In this mechanism D transfers an electron to A

through the bridge. The newly formed D⁺ and A[−] are then rapidly reduced and oxidized, respectively, at the electrodes, giving rise to a steady state in which the current depends on the rate of electron transfer from D to A, i.e.



where M_L and M_R denote the left and right electrodes. The rate constant for electron transfer from D to A is given by⁷

$$k_{\text{DA}} = A_{\text{DA}} \exp[-(\lambda_{\text{DA}} + \Delta G_{\text{DA}}^0)^2 / 4\lambda_{\text{DA}} k_{\text{B}} T] \quad (5)$$

where A_{DA} is a prefactor, λ_{DA} is the (vertical) reorganization energy and ΔG_{DA}^0 is the driving force for the intramolecular electron transfer.

Thermodynamic Considerations. The driving force is composed of field-independent and field-dependent terms. The first, ΔG_{c}^0 , is determined by the difference between the reduction potentials of the acceptor and donor couples

$$\Delta G_{\text{c}}^0 = -e\Delta E_{\text{DA}}^0 = -e(E_{\text{A/A}^-}^0 - E_{\text{D/D}^+}^0) \quad (6)$$

where e is the electronic charge, 1.60×10^{-19} coulomb (C). In practice, of course, one may start with fully oxidized or fully reduced DBA and the system may be symmetrical ($\Delta E_{\text{DA}}^0 = 0$) or unsymmetrical ($\Delta E_{\text{DA}}^0 > 0$ for downhill (exergonic) electron transfer).

The second contribution to the driving force, ΔG_{f}^0 , is the energy change deriving from the fact that the electron transfer is occurring in an electric field.¹² In the D-to-A transfer (eq 3) a charge e is moved a distance r , where r is the D–A separation, in the electric field created by the applied potential. If we treat the electrode assembly as a parallel-plate capacitor, the field is uniform and equal to V_{app}/d , where d is the electrode separation (a convenient, but not essential assumption). For $V_{\text{app}} = 1$ V and $d = 10$ Å the field is 10^7 V/cm, which is considerable. For current to flow from left to right, the applied voltage must place the donating (left) electrode at a higher energy (more negative

[†] Brookhaven National Laboratory.

[‡] Beckman Institute.

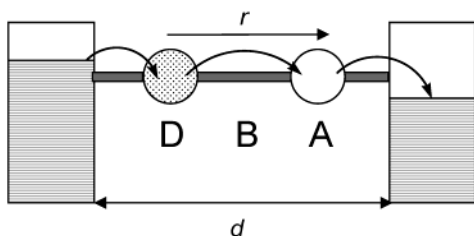


Figure 1. Donor-bridge-acceptor assembly attached to two metal electrodes separated by d . The D-A separation is r . The applied voltage V_{app} is such that electrons move from left to right.

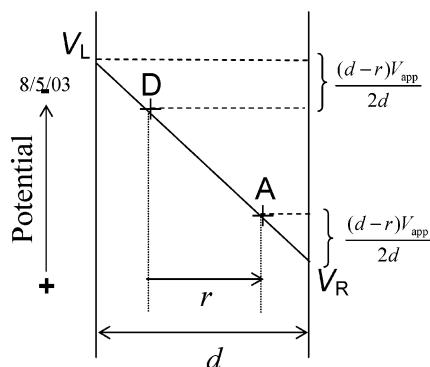


Figure 2. Contribution of the electric field to the redox thermodynamics. $V_{app} = V_R - V_L$.

potential) than D and the acceptor (right) electrode at a lower energy (more positive potential) than A. The energy change associated with moving the electron from the left to the right in the field is

$$\Delta G_f^0 = -eV_{app}r/d \quad (7)$$

(Equivalently, this energy change is given by the electronic charge multiplied by the difference in the electrostatic potential at the D and A sites.) As shown in Figure 2, the potential difference between D and the left electrode and between the right electrode and A is

$$V_{LD} = V_{AR} = (d-r)V_{app}/2d \quad (8)$$

when D-B-A is placed symmetrically in the electrode gap. The free-energy changes for steps 2-4 are thus given by

$$\Delta G_{LD}^0 = -e \left[(E_{D+/D}^0 - E_L^0) + \frac{(d-r)}{2d} V_{app} \right] - e \left[\left(E_{D+/D}^0 - \frac{r}{2d} V_{app} \right) - \left(E_L^0 - \frac{1}{2} V_{app} \right) \right] \quad (9a)$$

$$\Delta G_{DA}^0 = -e \left[(E_{A/A-}^0 - E_{D+/D}^0) + \frac{r}{d} V_{app} \right] = -e \left[\left(E_{A/A-}^0 + \frac{r}{2d} V_{app} \right) - \left(E_{D+/D}^0 - \frac{r}{2d} V_{app} \right) \right] \quad (9b)$$

$$\Delta G_{AR}^0 = -e \left[(E_R^0 - E_{A/A-}^0) + \frac{(d-r)}{2d} V_{app} \right] = -e \left[\left(E_R^0 + \frac{1}{2} V_{app} \right) - \left(E_{A/A-}^0 + \frac{r}{2d} V_{app} \right) \right] \quad (9c)$$

where E_L^0 and E_R^0 are the potentials corresponding to the Fermi levels of the left and right metal electrodes before the voltage is applied. For identical electrodes $E_L^0 = E_R^0$. Essentially, the donor becomes a more powerful reductant and the acceptor a

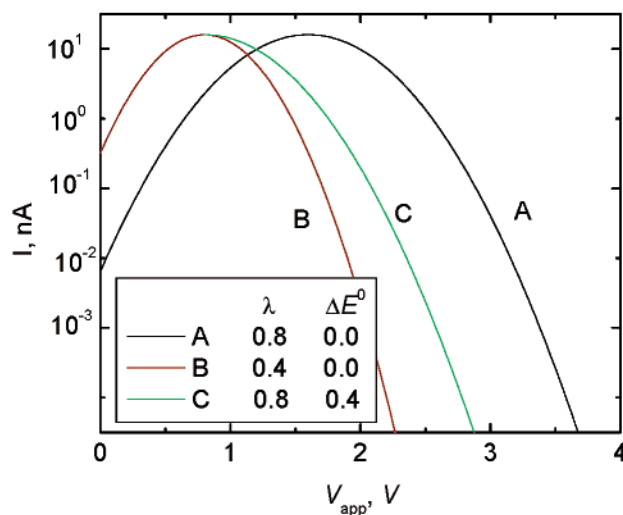


Figure 3. Current per DBA vs V_{app} for λ_{DA} and ΔE^0 values shown (λ in eV, $r/d = 0.5$, $A_{DA} = 10^{11} \text{ s}^{-1}$). The curves start at $V_{app} = 2\Delta E_{DA}^0$.

more powerful oxidant; the left electrode becomes more reducing, and the right electrode, more oxidizing when the voltage is applied. For regeneration, steps 2 and 4 must be thermodynamically favorable, e.g.

$$V_{app} \geq \left(\frac{d}{d-r} \right) \Delta E_{DA}^0$$

for the case when D and A are symmetrically located in the voltage gap $V_R - V_L$, i.e., $E_L^0 = E_R^0 = (E_{D+/D}^0 + E_{A/A-}^0)/2$.

Rates, Currents, and Conductances. Although we have focused above on the thermodynamic changes in the various steps, the steady-state current is determined by the absolute and relative rates of reactions 2-4. The overall three-step kinetic scheme is analogous to that for electron-transfer reactions in solution, in which any of the three steps can be rate-determining.^{13,14} Here we assume that the formation of D-B-A is rapid and essentially complete so that the current is determined by k_{DA} . At the steady state, the reverse of eq 3 for a downhill reaction (k_{AD}) is negligible and $k_{AR}, k_{LD} \gg k_{DA}$. The rate of forward electron transfer is then equal to the $(\text{Area})\Gamma_{DBA}k_{DA}$, where Γ_{DBA} is the surface concentration of DBA, and the current I per D-B-A is given by

$$I = ek_{DA} = 1.60 \times 10^{-19} k_{DA} \text{ amp} \quad (10)$$

where

$$k_{DA} = A_{DA} \exp[-(\lambda_{DA} - e(\Delta E_{DA}^0 + rV_{app}/d))^2/4\lambda_{DA}k_B T] \quad (11a)$$

$$A_{DA} = \frac{2\pi H_{DA}^2}{h} \left(\frac{\pi}{\lambda_{DA} k_B T} \right)^{1/2} \text{ s}^{-1} \quad (11b)$$

and H_{DA} is the D-A electronic coupling element at separation distance r .

In Figure 3, plots of the hopping current per D-B-A vs applied voltage are shown for a range of ΔE^0 and λ_{DA} values. Over the 4-volt range in applied voltage considered, the $\Delta E^0 = 0$; $\lambda_{DA} = 0.8$ curve (A) enters the inverted region at the highest applied voltage. Decreasing λ_{DA} and/or increasing ΔE^0 produces earlier entry into the inverted region. At $V_{app} = 2 \text{ V}$, just beyond A's current maximum, the currents for C and B are orders of magnitude smaller than that of A. It is clear that introduction

of asymmetry through increasing ΔE^0 renders the inverted region more readily accessible. The large reduction in k_{DA} (and I_{DA}) at high applied voltages is in striking contrast to the electron-transfer processes involving the metal, k_{LD} , k_{AR} , which are insensitive to the large driving forces because of the high density of metal states.

From eqs 10 and 11 the corresponding expression for the conductance $g = dI/dV = d(e k_{DA})/dV$ per D–B–A is

$$g = (e^2 r k_{DA} / d \lambda_{DA} k_B T) (\lambda_{DA} - e \Delta E_{DA}^0 - e r V_{app} / d) \quad (12)$$

(Note that when $\Delta G^0 = 0$, $k_{DA} = k_{AD} = k^0$ and the currents in the forward (right) and reverse (left) directions are equal. The net current is zero and $g^0 = e^2 r k^0 / d k_B T = 3.1 \times 10^{-9} (r/d) k^0$ nanoSiemens (nS) at room temperature.) As the applied potential is increased, the conductance changes continuously from positive through a maximum to negative. Negative differential conductance (inverted behavior) will be observed when $e(\Delta E_{DA}^0 + r V_{app} / d) > \lambda_{DA}$, a condition that is readily attainable, even for a symmetric system. The maximum and minimum in the conductance are at

$$V_m = \left(\frac{d}{er} \right) [(\lambda_{DA} - e \Delta E_{DA}^0) \mp (2 \lambda_{DA} k_B T)^{1/2}] \quad (13)$$

respectively. For A ($\lambda_{DA} = 0.8$ eV, $\Delta E_{DA}^0 = 0$), the current is the same (~ 10 nA) for an applied potential of 1.2 and 2.0 V, but the conductance changes from +24 to –24 nS.

In practice, the effect of the field on the electronic coupling element and on λ also needs to be considered.^{12,15,16}

As noted above, the electrode reactions do not show inverted behavior. Instead, the rate constants for electrode reactions plateau at^{17–19}

$$k_{LD} = P_{LD} = \frac{4\pi^2 \rho_L H_{LD}^2}{h} \quad k_{AR} = P_{AR} = \frac{4\pi^2 \rho_R H_{AR}^2}{h} \quad (14)$$

when $-\Delta G_{LD}^0 > 2\lambda_{D^+/D}$ and $-\Delta G_{AR}^0 > 2\lambda_{A/A^-}$, respectively. In the above expressions, ρ_L and ρ_R are the density of states in the left and right electrodes (assumed constant and continuous) and H_{LD} and H_{AR} are the electronic coupling elements between the left (right) electrode and the D (A) site. Provided that $\lambda_{D^+/D} = \lambda_{A/A^-} = \lambda_{DA}/2$, the rate constants for the electrode reactions level off when their driving forces equal λ_{DA} . Moreover, the electrode reactions attain half their maximum rate constant when the driving force is one-half λ_{DA} .²⁰ Evidently, the free-energy dependence of the electrode reactions is much smaller than that of the (intramolecular) D-to-A electron-transfer step. Further, if we assume that the electrodes are identical, $r/d = 0.5$, and that the coupling elements for the three steps have the same exponential distance dependence and the same values at contact of the sites, i.e., $\beta_{LD} = \beta_{AR} = \beta_{DA}$ and $H_{LD}^0 = H_{AR}^0 = H_{DA}^0$ in the free-energy regime of interest, the ratio of the maximum electron-transfer rate constants is

$$\frac{k_{LD}(\text{plateau})}{k_{DA}(\text{max})} = \frac{k_{AR}(\text{plateau})}{k_{AD}(\text{max})} = \frac{3.5\rho(\lambda_{DA} k_B T)^{1/2}}{\exp[-\beta r/2]} \quad (15)$$

which is greater than unity for $\rho = 0.27$ eV⁻¹ (Au electrode) when, for example, $\lambda_{DA} > 0.4$ eV and $\beta r > 5$.^{21–23}

Applications. To illustrate an approach to switching, we consider a pair of identical D–B–A assemblies attached to metal electrodes but oriented in opposite directions with respect to the local electric field (Figure 5). We compare the current

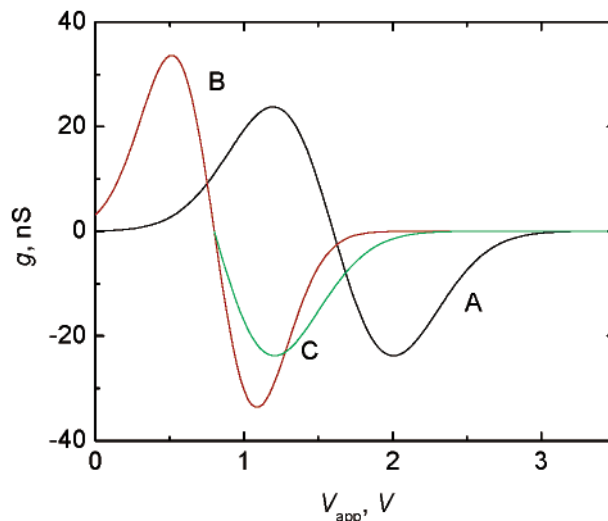


Figure 4. Conductance per D–B–A vs V_{app} for curves A–C in Figure 3.

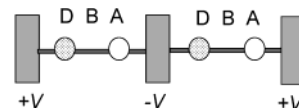


Figure 5. An M|D–B–A|M|D–B–A|M assembly designed to switch the current from the right branch to the left branch as the applied voltage is increased.

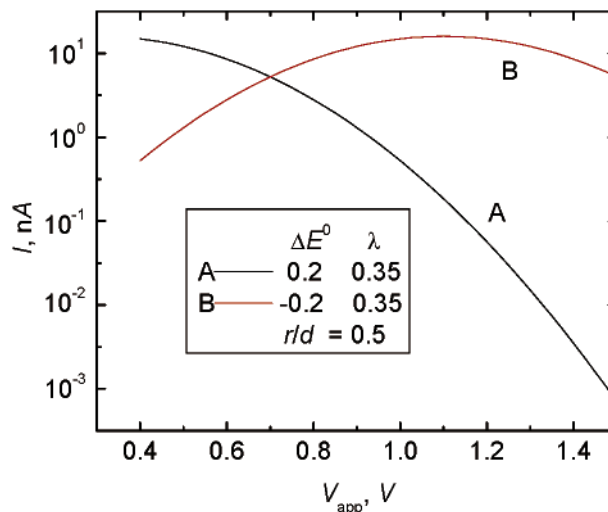


Figure 6. Comparison of currents through a single DBA (curve A) and single A⁻–B–D⁺ (curve B) as V_{app} increases.

toward the right through D–B–A and toward the left through A⁻–B–D⁺. For the case of the latter configuration at the steady state, the reverse of eq 3, A⁻–B–D⁺ → A–B–D, k_{AD} , is rate-determining. Because this reaction is intrinsically uphill, $V_{app} \geq (d/r)|\Delta E_{DA}^0|$ is required to render it thermodynamically favorable.²⁴ The ratio of the currents through A⁻–B–D⁺ and D–B–A is

$$I_{ABD}/I_{DBA} = \exp[e \Delta E_{DA}^0 ((r/d)e V_{app} - \lambda_{DA}) / \lambda_{DA} k_B T] \quad (16)$$

and the currents through the two branches are equal for

$$e V_{app} = (d/r) \lambda_{DA} \quad (17)$$

As shown in Figure 6, for $\lambda_{DA} = 0.35$ eV, $r/d = 0.5$, and $\Delta E^0 = \pm 0.2$ V, the currents through D–B–A and A⁻–B–D⁺

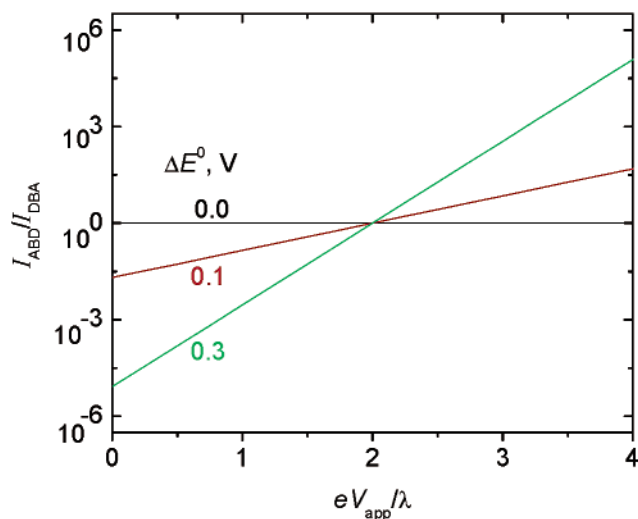


Figure 7. Ratio of currents through DBA and A^-B-D^+ as a function of eV_{app}/λ_{DA} for $\Delta E^0_{DA} = 0.0, 0.1$, and 0.3 V and $r/d = 0.5$.

are equal at $V_{app} = 0.7$ V. Shifting V_{app} symmetrically about this crossing-point by moving from $V_{app} = 0.45$ V to $V_{app} = 0.95$ V, decreases the current through D–B–A by an order of magnitude and increases the current through A^-B-D^+ by the same factor. Effectively, the current is switched from the right branch to the left branch with a more than 100-fold change in the ratio of the currents. Of course, the hopping current through both branches will be turned off at sufficiently large applied voltage as the $A-B-D$ electron transfer becomes increasingly inverted. However, other hopping mechanisms (for example, involving reduction of a molecular bridge) or tunneling processes could become important under these conditions.

The dependence of the current ratio on ΔE^0_{DA} and V_{app}/λ_{DA} is presented in Figure 7. It is apparent that efficient switching can be achieved at moderate applied potentials through use of an unsymmetrical D–B–A composed of redox centers with small λ_{DA} values. The maximum (and minimum) conductance, which is proportional to $\lambda_{DA}^{-1/2}$ (eq 18, where $k_{g,m} = A_{DA}e^{-1/2}$, is obtained by substituting eq 13 into eq 12)

$$g_m = \pm \left[\frac{e^2 r k_{g,m}}{d \sqrt{2 \lambda_{DA} k_B T}} \right] \quad (18)$$

provides a measure of the switchability of a given system whereas the range over which the system will be operable is determined by $\lambda_{DA}^{1/2}$ (eq 13). Thus, systems with small λ_{DA} values are readily switched but carry large currents only over a narrow range of applied voltage.

Although our discussion has been restricted to single D–B–A $^-$ assemblies, extension of this approach to bilayer films and to applications in very small circuits is obvious. The effect of the field on the reorganization energy could be amplified by combining normal and inverted D–B–A systems in networks and through use of paired self-assembled mono-

layers. In practice, the transfer from D to A can be outer sphere, with the bridge being the surrounding material or vacuum. In another interesting direction, semiconductor nanocrystals²⁵ might replace the molecular D, B, and A moieties.

Acknowledgment. This research was carried out at Brookhaven National Laboratory under contract DE-AC02-98CH10886 with the U.S. Department of Energy, supported by its Division of Chemical Sciences, Office of Basic Energy Sciences, and at the California Institute of Technology by the Arnold and Mabel Beckman Foundation. We are indebted to S. W. Feldberg and R. A. Marcus for invaluable discussions.

References and Notes

- (1) Aviram, A.; Ratner, M. A. *Chem. Phys. Lett.* **1974**, *29*, 277–283.
- (2) Ratner, M. A.; Davis, B.; Kemp, M.; Mujica, V.; Roitberg, A.; Yaliraki, S. *Ann. N. Y. Acad. Sci.* **1998**, *852*, 22–37.
- (3) Ratner, M. A.; Jortner, J. In *Molecular Electronics*; Ratner, M. A., Jortner, J., Eds.; Blackwell: Oxford, U.K., 1997; pp 5–72 (see also references therein).
- (4) Nitzan, A.; Ratner, M. A. *Science* **2003**, *300*, 1384–1389.
- (5) Reed, M. A.; Zhou, C.; Muller, C. J.; Burgin, T. P.; Tour, J. M. *Science* **1997**, *278*, 252–254.
- (6) Tian, W.; Datta, S.; Hong, S.; Reifenberger, R.; Henderson, J. I.; Kubiak, C. P. *J. Chem. Phys.* **1998**, *109*, 2874–2882.
- (7) Marcus, R. A.; Sutin, N. *Biochim. Biophys. Acta* **1985**, *811*, 265–322.
- (8) Adams, D.; Brus, L.; Chidsey, C. E. D.; Creager, S.; Creutz, C.; Kagan, C. R.; Kamat, P. V.; Lieberman, M.; Lindsay, S.; Marcus, R. A.; Metzger, R. M.; Michel-Beyerle, M. E.; Miller, J. R.; Newton, M. D.; Rolison, D. R.; Sankey, O.; Schanze, K. S.; Yardley, J.; Zhu, X. *J. Phys. Chem. B* **2003**, *107*, 6668–6697.
- (9) Segal, D.; Nitzan, A.; Davis, W. B.; Wasielewski, M. R.; Ratner, M. A. *J. Phys. Chem. B* **2000**, *104*, 3817–3829.
- (10) Segal, D.; Nitzan, A.; Ratner, M.; Davis, W. B. *J. Phys. Chem. B* **2000**, *104*, 2790–2793.
- (11) Mujica, V.; Nitzan, A.; Datta, S.; Ratner, M. A.; Kubiak, C. P. *J. Phys. Chem. B* **2003**, *107*, 91–95.
- (12) Galoppini, E.; Fox, M. A. *J. Am. Chem. Soc.* **1996**, *118*, 2299–2300.
- (13) Newton, M. D.; Sutin, N. *Annu. Rev. Phys. Chem.* **1984**, *35*, 437–480.
- (14) Sutin, N. *J. Photochem. Photobiol., A* **1979**, *10*, 19–40.
- (15) Gao, Y. Q.; Marcus, R. A. *J. Phys. Chem. A* **2002**, *106*, 1956–1960.
- (16) Franzen, S.; Lao, K.; Boxer, S. G. *Chem. Phys. Lett.* **1992**, *197*, 380–388.
- (17) Chidsey, C. E. D. *Science* **1991**, *251*, 919–922.
- (18) Gosavi, S.; Marcus, R. A. *J. Phys. Chem. B* **2000**, *104*, 2067–2072.
- (19) Feldberg, S. W.; Newton, M. D.; Smalley, J. F. In *Electroanalytical Chemistry Series*; Bard, A. J., Rubinstein, I., Eds.; Marcel Dekker: New York (in press).
- (20) Feldberg, S. W. Personal communication.
- (21) The value of $H^0_{Au,Fe}$ for a ferrocene linked to a gold electrode via a sulfur atom attached to the cyclopentadienyl ring has been estimated as 0.76 eV,²² larger than $H^0_{Fc,Fe}$ calculated for a covalently linked ferrocene–ferrocenium pair.²³ Such a pattern would further accelerate the electrode-based reactions over the D-to-A electron transfer.
- (22) Smalley, J. F.; Finklea, H. O.; Chidsey, C. E. D.; Linford, M. R.; Creager, S. E.; Ferraris, J. P.; Chalfant, K.; Zawodzinski, T.; Feldberg, S. W.; Newton, M. D. *J. Am. Chem. Soc.* **2003**, *125*, 2004–2013.
- (23) Newton, M. D. *Chem. Rev.* **1991**, *91*, 767–792.
- (24) Even if the $A^-B-D^+ \rightarrow A-B-D$, k_{AD} , transfer (eq 3) is thermodynamically uphill, the reverse electron transfer can be neglected when oxidation of newly formed D at the far left anode or the reduction of A at the cathode (central electrode) is sufficiently rapid.
- (25) Nirmal, M.; Brus, L. E. *Acc. Chem. Res.* **1999**, *32*, 407.